MicroRNA-718 inhibits mitochondrial fusion and ameliorates IMQ-induced psoriasis inflammation mediated by PHB and STAT1

Himani Rani
Academy of Scientific & Innovative Research (AcSIR)
Neeru Saini
nkhanna@igib.res.in
Academy of Scientific & Innovative Research (AcSIR)

Research Article

Keywords: MiR-718, Psoriasis, JAK/STAT signaling, Imiquimod, Mitochondrial dynamics, keratinocytes

Posted Date: July 1st, 2024

DOI: https://doi.org/10.21203/rs.3.rs-4557621/v1

Additional Declarations: No competing interests reported.

Abstract

Multiple inflammatory pathways contribute to the development of psoriasis, leading to the hyperproliferation and dedifferentiation of keratinocytes at the affected site. The precise etiology of psoriasis pathogenesis remains unclear. Given that a single miRNA can regulate a cellular process involving multiple genes, there has been a rise in miRNA-based therapy studies over the past few decades. The current study aimed to investigate the therapeutic potential of miR-718 overexpression in treating psoriasis and to elucidate its underlying mechanisms using an imiquimod (IMQ)-induced mouse model and human keratinocytes (HaCaT). Additionally, the drug tofacitinib was incorporated in the *in-vivo* study to provide further insights. We observed that miR-718 overexpression leads to the inhibition of JAK/STAT signaling, as evidenced by the reduced expression of STAT1, JAK1, JAK2, and JAK3, directly inhibiting STAT1, both *in-vitro* and *in-vivo*. Moreover, the expression of STAT2 and STAT3 was also found to be downregulated in *in-vitro*studies. *In-vivo* studies further show that miR-718 decreases the NF-kB, critical mediators of inflammation, upon ectopic expression in psoriatic mice. Immunohistochemistry (IHC) results indicate reduced acanthosis and parakeratosis in IMQ-induced psoriatic mice, potentially resulting from halted JAK/STAT signaling. In the miR-718 transfected mice skin, there was decreased expression of VEGF and matrix metalloproteases (MMP7 and MMP9), as shown by IHC and western blotting, respectively. The study also demonstrated that miR-718 represses mitochondrial fusion by inhibiting MFN1, MFN2, PHB, and OPA1 in HaCaT cells, while increasing DRP1 expression. Understanding the mechanism by which miR-718 ameliorates psoriasis not only provides new insight but also raises hopes for translating miR-718 as potential therapeutic agent for psoriasis.

1. Introduction

Psoriasis, one of the most prevalent autoimmune skin conditions, involves both innate and adaptive immunity. Its estimated prevalence varies depending on geographic distribution, age, and ethnicity, ranging from 0.44–2.8% in India and 0.5–11% worldwide (1). The condition is characterized by red, raised, inflammatory skin patches that can develop whitish-silver scales or plaques. The overproduction of inflammatory cytokines and dysregulation of cellular signal transduction are recognized as hallmarks of psoriasis, leading to inflamed skin patches. Additionally, keratinocytes proliferate uncontrollably, differentiate dysfunctionally, and leukocytes infiltrate psoriatic sites (2). Apart from physical trauma, psoriasis has been associated with depression, social stigmatization, and other psychiatric illnesses in patients. Various forms of psoriasis are reported depending on their location, affected area, and manifestations (3).

Although the exact pathogenesis of psoriasis remains unclear, the role of IL-23/Th17 axis is believed to be predominant in this chronic inflammatory disease and it is best treatable with IL-23/Th17-based approaches (4). Activated skin resident dendritic cells drive the differentiation of T-cells into Th17 and Th1 cells, mediated by IL-23 and IL-12, respectively. The Th17 pathway produces IL-17A, IL-17F, and IL-22, while the Th1 pathway secretes IFN-γ, further leading to keratinocyte proliferation through activated intracellular signaling and transcription pathways (5). Janus kinases (JAKs) are tyrosine kinases connected noncovalently to cytokine receptors, triggering the signal transducer and activator of transcription (STAT) pathway. Activation of JAKs results in the phosphorylation of STAT monomers, leading to dimerization, nuclear translocation, and transcription of proinflammatory genes (6). This inflammatory cascade at the psoriatic site promotes the invasion of immune cells through induction of angiogenesis and endothelial adhesion molecules. Increased expression of STAT1, STAT2, and STAT3 and their activated forms have been observed in lesional psoriatic skin compared with non-lesional skin (7–9).

Recent scientific advances have associated mitochondrial dynamics with inflammatory responses, showing interactions with both innate and adaptive immune cells (10). Decreased mitochondrial fusion and increased fission have been implicated in multiple aspects of inflammatory responses in several human diseases (11, 12). Furthermore, reports highlight the involvement of mitochondrial reactive oxygen species (mROS) in regulating mitochondria-mediated inflammatory signaling (13).

Multiple treatments, including oral agents, phototherapy, and biological substances, are available for moderate to severe psoriasis. Biologics, which have the highest efficacy, belong to four classes: IL-12/23 inhibitors, IL-23 inhibitors, IL-17 inhibitors, and TNF inhibitors. Since psoriasis is an autoimmune inflammatory disease, tofacitinib and baricitinib have shown improvement by inhibiting JAK/STAT signaling. Despite these therapies, psoriasis can recur, and treatments may have unacceptable adverse effects (14).

Considerable advances have been made in understanding the molecular pathogenesis of psoriasis, particularly regarding microRNAs (miRNAs) over the past two decades. miRNAs are evolutionarily conserved, ~ 22 nucleotides long single-stranded non-coding RNAs that regulate gene expression at the post-transcriptional level by base pairing with complementary regions of target mRNA. Various miRNAs have been implicated in psoriasis pathogenesis, including miR-31, miR-21, miR-210, miR-126, and miR-33, each influencing different aspects of the immune response and cellular processes involved in psoriasis (15–18).

Previously, our lab identified significant differential expression of miR-718 in PUVA treated HaCaT cells using miRNA microarray and qRT-PCR methods (19). However, to date, the role of miR-718 in psoriasis remains unexplored. In this study, we demonstrate the resolution of psoriatic inflammation through the overexpression of miR-718, which inhibits STAT1 and PHB. These proteins are involved in crucial inflammatory processes, specifically the JAK/STAT signaling pathway and mitochondrial fusion. Collectively, these findings underscore the potential of miR-718 as a novel therapeutic intervention for psoriasis.

2. Results

2.1. Insilico-analysis of miR-718

To delve into the biological role of miR-718 in psoriasis, we utilized two independent target prediction tools, TargetScan and miRWalk, to predict its target genes (20, 21). Concurrently, we extracted psoriasis-related genes from the MalaCards database (22). Comparison of the predicted target gene list with the MalaCards retrieved 70 genes that were common (Fig. 1a). PubMed analysis revealed that most of these genes are involved in psoriasis-related signaling pathways and can be categorized into six groups (references are given in supplementary Table 1): proliferation, inflammation, lipid metabolism, disease susceptibility, adhesion and differentiation, and angiogenesis (Fig. 1b).

Functional annotation of these common genes using Panther pathway analysis unveiled enrichment of pathways such as the JAK-STAT signaling pathway, p53 signaling pathway, and IFN-gamma signaling pathway, all of which are known to be associated with inflammation (23). Interestingly, we observed that the STAT1 gene plays an important role in most of these pathways (Fig. 1c). However, the functional relevance of miR-718 in regulating intracellular STAT1 has not been explored. Therefore, we aimed to validate the interaction between STAT1 and miR-718 and investigate the role of their interaction in psoriasis using *in-vivo* and *in-vitro* studies.

2.2. miR-718 overexpression inhibits JAK1/STAT1 protein expression in human keratinocytes

To evaluate the effect of miR-718, human keratinocytes (HaCaT cells) were transfected with either miR-718 or AM-718 or their respective controls. Interestingly, quantitative RT-PCR analysis using miR-718 specific primers revealed a significant increase in the levels of mature miR-718 by 12.1-fold ($p = 0.005$) (Fig. 2a) and a significant decrease in miR-718 levels after AM-718 treatment (Fig. 2b) in HaCaT cells compared to negative controls.

Next, we examined STAT1 expressions at the transcriptional and translational levels. Overexpression of miR-718 led to a decrease in STAT1 mRNA levels by 0.41-fold ($p = 0.21$), while AM-718 treatment increased STAT1 mRNA levels by 5.13-fold ($p = 0.05$) in HaCaT cells (Fig. 2c). Overexpression of miR-718 led to the downregulation of STAT1 protein by 0.23-fold ($p = 0.01$), while silencing of miR-718 using AM-718 upregulated STAT1 protein expression by 1.3-fold ($p = 0.03$) (Fig. 2f) in human keratinocytes (HaCaT). Phosphorylated forms of STAT1 at its regulatory sites, Ser727 and Tyr701, were also examined by western blotting analysis. They were found to be decreased upon miR-718 overexpression and significantly increased upon AM-718 treatment by 1.74-fold ($p = 0.01$) and 1.12-fold ($p = 0.007$) respectively (Fig. 2g, 2h) in HaCaT cells.

At the translational level, JAK1 expression was found to be downregulated in miR-718 transfected cells and upregulated in AM-718 transfected cells compared with their respective negative controls (Fig. 2d), although the results were not significant. However, the expression of phosphorylated Jak1 (pJak1) was significantly decreased ($p = 0.03$) upon miR-718 overexpression (Fig. 2e) in HaCaT cell line.

Cytokeratin 17 (K17) is known to be overexpressed in the epidermis of psoriatic sites but absent in the epidermis of healthy skin. The overexpression of K17, caused by IL-17A, involves both the STAT1 and STAT3 pathways (24, 25). Herein, we found that miR-718 inhibited the expression of K17 protein in HaCaT cells (Fig. 2i). These results collectively indicate that miR-718 significantly reduces JAK1/STAT1 proteins/phosphorylation and inhibits K17 expression, a hallmark of psoriasis, in human keratinocytes (HaCaT).

2.3. Effect of miR-718 on other JAK/STAT pathway related proteins in HaCaT cells

The JAK/STAT intracellular signaling pathway involves different JAKs and STATs within the cell. Herein, we investigated the effect of differential expression of the STAT1 on other important molecules in the JAK/STAT signaling pathway using miR-718 in HaCaT cells. Our results showed that the protein expression of JAK2, JAK3, and phosphorylated JAK2&3 in miR-718 transfected cells were significantly

reduced by 0.26-fold (p = 0.03), 0.14-fold (p = 0.1), and 0.39-fold (p = 0.03) respectively, compared to their negative control (M-NC) cells. Furthermore, their expression was found to be reversed by using AM-718 (Fig. 3a-c).

Additionally, increased protein expression of STAT2 and STAT3 is found in psoriatic skin lesions compared to non-lesional psoriatic skin (7, 9). 24hr post transfection of miR-718 in HaCaT cells showed decreased protein levels of STAT2 and STAT3 by 0.42-fold (p = 0.006) and 0.16-fold (p = 0.03) respectively (Fig. 3d,e), and inhibiting miR-718 using AM-718 increased the STAT2 and STAT3 protein levels. While the phosphorylated STAT3 (Tyr705) levels were insignificantly increased upon both miR-718 and AM-718 treatment by 1.15-fold (p = 0.07) and 1.18-fold (p = 0.07) in HaCaT cells (Fig. 3f). All these results indicate that miR-718 alters JAK/STAT pathway proteins, albeit at different levels, in HaCaT cells.

2.4. miR-718 overexpression inhibits JAK/STAT1 signaling in IMQ-induced psoriatic mice model

To assess the physiological relevance of miR-718, we established an IMQ-induced psoriasis mice model using topical treatment of IMQ for consecutive 5 days, as described in Materials and Methods. Subsequent intradermal injections of miR-718/M-NC were administered according to the depicted timeline as shown in Fig. 4a. We consistently observed that on day 2, except for the vaseline mice group, all other groups exhibited modest erythema, which worsened on day 3 with the appearance of white scales. Additionally, the thickness of the local skin was found to be greater than that of normal skin, clearly demonstrating the efficacy of the psoriatic model (Supplementary Fig. 1a). There was a significant increase (2.7-fold, p = 8.17e-08) in spleen size at the end of the study following 5 days of IMQ administration (Supplementary Fig. 1b). Treatment with miR-718 alleviated the psoriasis-like symptoms in mice.

To investigate the underlying mechanisms of miR-718 on IMQ-induced psoriasis mice, we assessed the expression of JAK/STAT1 signaling and its possible downstream signaling. Western blot analysis of JAK1, JAK2, JAK3, and their phosphorylated forms was performed in miR-718 transfected mice and IMQ-induced psoriasis mice skin tissues. We found decreased protein expression of JAK1, JAK2, JAK3, and pJAK2&3 compared to IMQ-mice (Fig. 4b-f), showing a similar pattern to that observed in HaCaT cells. The results of JAK2 and pJAK2&3 protein expression were significant. Next, we examined the direct target of miR-718, STAT1 protein expression, and its downstream-related protein NF-kB. Western blotting results revealed lower expression of STAT1, pSTAT1, NF-kB, and pNF-kB in the miR-718 treated mice group compared with the M-NC treated mice group (Fig. 4h-k). All these findings showed that miR-718 was able to downregulate the JAK/STAT signaling and its related processes in the mice model as well.

2.5. Alteration of different psoriatic biomarkers due to upregulation of miR-718 in mice psoriatic skin

Hematoxylin and eosin (H&E) staining revealed acanthosis on the back skin (indicated by the yellow double-headed arrow in Fig. 5ai) of IMQ-treated mice, likely caused by hyperproliferation of keratinocytes. Cutaneous scaling, often indicating parakeratosis or abnormal epidermal differentiation, a common feature of psoriasis lesions, was observed in the IMQ-treated mice (indicated by the red arrow in Fig. 5ai), which was reversed in skin treated with miR-718. Furthermore, IMQ-treated animals lacked the granular layer seen in vaseline treated mice but could be observed in miR-718 treated mice.

Hyperproliferation of keratinocytes was demonstrated by studying the expression of the Ki67 marker (Fig. 5bi). Ki67 was strongly expressed in both the spinosum layer and the basal layer, with greater density in the IMQ mice group. Compared with the IMQ group, the expression of Ki67 in the miR-718 and tofacitinib (widely used anti-psoriatic drug) treated group was significantly reduced. Moreover, the epidermis of mice treated with vaseline displayed normal expression of involucrin, a hallmark of terminal keratinocyte development, in the upper stratum spinosum, whereas the epidermis of animals treated with IMQ showed more widespread expression of involucrin. Involucrin expression was reduced in the miR-718 treated group compared with the IMQ mice group (Fig. 5aii).

An overexpression of VEGF can result in a psoriasiform phenotype, characterized by parakeratosis, acanthosis, dilated and convoluted dermal blood vessels, and epidermal microabscesses as shown in Fig. 5bii. Quantification of Ki67 and VEGF immunohistochemistry staining intensity using Fiji software demonstrated that miR-718 inhibited proliferation and angiogenesis in the miR-718 treated mice group. Furthermore, matrix metalloproteinases (MMPs) are also known to induce structural alterations in the epidermis, stimulating angiogenesis in dermal blood vessels and resulting in immune cell infiltration in psoriasis (26). Using western blot analysis, we also found an inhibitory effect of miR-718 on MMP9 and MMP7 after miR-718 treatment. Additionally, immunohistochemistry results demonstrated lesser invasion of CD4 positive cells in the miR-718 treated mice group (Supplementary Fig. 1c). Overall, our findings suggest that miR-718 has immense therapeutic potential for the treatment of psoriasis.

2.6. Role of miR-718 overexpression on mitochondrial dynamics in HaCaT cells

Mitochondrial dynamics play a crucial role in exacerbating inflammation associated with psoriasis. Therefore, we investigated the effect of miR-718 on mitochondrial dynamics through its direct target, the PHB gene, which is known to control mitochondrial dynamics (27). We observed a significant downregulation of the PHB gene by 0.33-fold ($p = 0.03$) due to miR-718 overexpression and an upregulation of the PHB gene upon silencing of miR-718 using AM-718 at the translational level (Fig. 6b). Furthermore, inhibition of MFN1 by 0.11-fold, MFN2 by 0.13-fold, and OPA1 by 0.09-fold ($p = 0.004$) proteins, along with an upregulation of DRP1 by 1.2-fold ($p = 0.09$) protein, confirmed the halting of mitochondrial fusion and the presence of mitochondrial fission in miR-718 transfected HaCaT cells. Additionally, 24hr post transfection of AM-718 treatment promoted the expression of proteins MFN1 by 1.22-fold, MFN2 by 1.47-fold ($p = 0.002$), and OPA1 by 1.18-fold ($p = 0.06$), while inhibiting the mitochondrial fission regulation protein, DRP1 by 0.22-fold (Fig. 6b-e). As shown in Fig. 6g, PHB was proved to be a target of miR-718 using a dual luciferase reporter assay.

Mitochondrial potential is also required to maintain interconnected and elongated mitochondria for the mitochondrial fusion process (28). Figure 6h depicts that miR-718 treatment led to depolarization of cells, indicated by a decreased red/green ratio, suggesting miR-718 mediated mitochondrial fusion. In summary, these results indicate that miR-718 inhibits mitochondrial fusion and promotes mitochondrial fission by directly targeting PHB.

3. Discussion

In humans, an overactivated skin immune system results in chronic inflammation, leading to psoriasis. This long-lasting inflammation is influenced by various factors such as lifestyle, obesity, genetic predisposition, environment, drugs, and associated comorbidities. While there are multiple treatments available targeting different key cytokines or cell receptors involved in inflammation processes in psoriasis, their adverse effects and the recurrence of the disease indicate the need for more effective therapeutic approaches. MicroRNA-based therapy has shown promise in clinical trials (29–31).

As depicted in the schematic representation, our study highlights the role of miR-718 in resolving inflammation by targeting two crucial inflammation-mediated processes: JAK/STAT signaling (by directly inhibiting STAT1) and mitochondrial dynamics (by directly targeting PHB). Administration of miR-718 in IMQ-induced psoriasis mice resulted in the resolution of psoriatic-like symptoms, such as skin thickening, desquamation, angiogenesis, and immune cell infiltration (as illustrated in Fig. 7). These findings suggest the potential of miR-718 as a candidate for improving psoriasis-related skin inflammation in patients.

MiR-718 has been reported as an anti-inflammatory and anti-proliferative regulator by directly targeting PTEN (32), suppressing the innate immune response in macrophage cells, and targeting VEGF in ovarian cancer studies (33). However, no study to date has explored the role of miR-718 in inflammation related to psoriasis. In this study, we conducted in-silico analysis to investigate the importance of studying miR-718 in JAK/STAT signaling in psoriasis, followed by validation in HaCaT cell line and IMQ-induced psoriasis mice models.

Our data demonstrate that overexpression of miR-718 downregulates STAT1, known to regulate genes involved in various cellular processes such as inflammation, proliferation, and keratinocyte differentiation. Interestingly, we observed changes in the expression of JAK1, JAK2, and JAK3 along with STAT1, both *in-vivo* and *in-vitro*, upon miR-718 overexpression. Protein expression of STAT2 and STAT3 was also reduced in miR-718 transfected cells *in-vitro*. Additionally, we found reduced expression of NF-kB/pNF-kB, predominantly regulated by JAK/STAT, in miR-718 treated mice compared to controls, indicating the potential role of miR-718 in regulating the JAK/STAT signaling pathway, a crucial inflammatory pathway in psoriasis.

Furthermore, we discovered a novel finding in this study regarding how inhibition of the PHB gene using microRNA could modulate mitochondrial dynamics in psoriasis. Kim et al. (2007) reported a dual role of PHB in psoriasis. The loss of function of the PHB gene in the basal layer of psoriatic skin has been identified as a negative regulator of the cell cycle, controlling proliferation in HaCaT keratinocytes. Additionally, PHB has been shown to modulate mitochondrial activity by maintaining its integrity (34). This study focuses on how the upregulation or downregulation of miR-718 could alter mitochondrial dynamics mediated by the PHB gene, which might further affect inflammation in psoriasis.

We validated PHB as a direct target of miR-718 and found downregulation of MFN1, MFN2, and OPA1 proteins upon miR-718 overexpression in HaCaT cells (Fig. 7). Inhibition of mitochondrial fusion protein could lead to mitochondrial fission, as confirmed by DRP1 protein expression and mitochondrial inner membrane potential calculation using JC-1 dye. Mitochondria have been implicated in psoriatic chronic inflammation. IL-17A-dependent inflammation could be resolved by inhibiting mitochondrial translation, which reduces

the expression of cytochrome c oxidase in T cells (35). However, the exact mechanism by which alterations in mitochondrial dynamics by miR-718 lead to the reduction of inflammation requires further examination.

In conclusion, our data suggest that miR-718 has dual functions in psoriasis: as a negative regulator of JAK/STAT signaling for the inflammation process and in regulating mitochondrial dynamics. Whether the dual functions of miR-718 are directly interconnected or signify two distinct mechanisms has not yet been investigated. Our findings represent an essential step towards the application of miR-718 as a potential therapeutic agent for psoriasis.

4. Material and methods

4.1. Cell Culture and treatments

The human keratinocyte cell line (HaCaT cells) was purchased from the National Centre for Cell Sciences (NCCS) in Pune, India, and cultured in DMEM F-12 media supplemented with 10% (v/v) fetal bovine serum, 100 Units/ml penicillin, and 100 mg/ml streptomycin at 37°C in a humidified atmosphere with 5% CO2. Cells were seeded in either 6-well or 12-well plates for subsequent growth and treatments. Reverse transfections were performed at 70–80% confluency using a miR-718 mimic (miR-718) and a miR-718 inhibitor (assay ID MC16440, THERMO Fisher Scientific, MA, USA) (AM-718) at 40 nM, with transfection reagent Fugene HD, and compared with their respective negative controls, miR negative control (M-NC) or anti-miR negative control (AM-NC). Cells were trypsinized and harvested 24 hours after transfection, then stored at -80°C until further use.

4.2. Total RNA isolation and Real-time quantitative PCR

Total RNA was extracted from HaCaT cells transfected with either 40nM of miR-718 or AM-718, or their respective negative controls, using TRIzol reagent (Invitrogen, Paris, France) according to the manufacturer's protocol. RNA quantification was performed on a NanoDrop spectrophotometer (ND1000, NanoDrop Technologies, Inc., Wilmington, USA). Total RNA (1 µg) was reverse transcribed using RevertAid H Minus Reverse Transcriptase (Fermentas, Glen Burnie, MD), and qRT-PCR was carried out in a 10 µL reaction volume using 2X SYBR Green master mix (Applied Biosystems-ABI, Foster City, CA) following the manufacturer's instructions. The real-time PCR data were analyzed using Pfaffl's method. The sequences of primers used for detecting the expression levels of STAT1 and 18S rRNA are listed in Table 1.

Table 1
List of Primer sequences used for experiments in the study.

Gene	Forward Primer 5'-3'	Reverse Primer 5'-3'
STAT1	ATGGCAGTCTGGCGGCTGAATT	CCAAACCAGGCTGGCACAATTG
18S	AGAAACGGCTACCACATCCA	CCCTCCAATGGATCCTCGTT
PHB 3'UTR	AGTTCACACACACCTGTTTCATCTGGTCACACAGTTAAAGAG	CTCTTTAACTGTGTGACCAGATGAAACAGGTGTGTGTGAACT

4.3. Mice and treatment

All animal protocols were approved by the Institutional Animal Ethics Committee of CSIR-Institute of Genomics and Integrative Biology, New Delhi, India. We developed an IMQ-induced psoriasis mice model using male C57BL/6 mice. The mice were fed a high-fat diet (HFD; D12492, Research Diets. Inc., NJ, USA) for 7 weeks, as HFD mice are more susceptible to developing severe psoriasis than chow diet-fed mice upon topical treatment with IMQ. Four-week-old male C57BL/6 mice were purchased from Livon Biolabs (Bengaluru, India) and housed in cages under a 12-hour alternating dark and light period. The mice were randomly divided into the following groups (5 mice in each group): Untreated mice group, IMQ mice group, vaseline mice group, miR-718 mice group, Scramble control mice group, and Tofacitinib mice group. Except for the untreated and vaseline groups, 62.5 mg of 5% IMQ cream was evenly applied to the exposed skin on the back of the mice. Synthetic miR-718 or scramble oligonucleotides (7 µg [Dharmacon Inc. (CO, USA)]) packed in the in vivo transfecting agent (Max Suppressor-In Vivo RNA-LANCEr II, Bioo Scientific, Austin, Tex) were injected intradermally into the shaved back skin of the mice once a day. Tofacitinib was administered in two doses 6 hours apart for a total dose of 30 mg/kg. Digital photography was used to record the changes in skin lesions at the same time every day. On the 5th day, mice were sacrificed 24 hours after the last treatment. The spleen and back skin of the mice were collected, fixed with 4% formalin, and stored at room temperature, while other tissues were stored at -80 °C. The spleen was used to calculate the spleen index using the formula: Spleen index = spleen weight (mg)/body weight (g).

4.4. Protein preparation and western blotting

The user lysed transfected cells with RIPA lysis buffer (50 mM Tris–HCl, pH 7.4, 150 mM NaCl, 1% NP40, 0.25% Na-deoxycholate, 1 mM EDTA) containing protease and phosphatase inhibitors (G-Biosciences, MO, USA) for 30 min on ice. The lysates were centrifuged at 16,000 g for 30 min at 4°C, and the supernatant was obtained. Protein concentration was estimated by the BCA method (Sigma, USA). Equal amounts of proteins (50–100 µg) were separated on 10% sodium dodecyl sulphate polyacrylamide gel electrophoresis (SDS-PAGE) and transferred to a PVDF membrane (Mdi; Advanced Microdevices, India). The membrane was blocked using 5% Bovine serum albumin (BSA) or 5% Skim milk (SM) for 2h at room temperature and then incubated with the respective antibodies in 2.5% BSA/ for 16 h at 4°C. The blot was washed three times using TBST and further incubated with the suitable secondary antibody for 1 h at room temperature. Antibodies used included STAT1, STAT2, STAT3, pSTAT1(Ser 727), and pSTAT1(Tyr727) from Affinity Biosciences (1:1000); PHB, NF-kB, pNF-kB, and cytokeratine 17 (K17) from Santa Cruz (1:200); MMP7 and MMP9 from Elabscience (1:1000); MFN1, MFN2, DRP1, and OPA1 from Cell Signaling Technology (CST) (1:1000); JAK1, JAK2, JAK3, pJAK1, and pJAK2&3 from Thermo Fisher Scientific (1:1000); Loading control β-actin from Abcam (Cambridge, UK) and GAPDH from CST (1:5000). The secondary antibodies were HRP-linked and used at 1:5000 concentration, and blots were developed using enhanced chemiluminescence (Thermo Fisher Scientific, CA, USA). Image Lab software was used to acquire and analyze images from specific Bio-Rad imaging systems.

4.5. Immunohistochemistry

The Ultra-Vision Quanto Detection Kit (Thermo Scientific, Waltham, MA, USA) was used according to the manufacturer's instructions. Skin biopsies were fixed in 10% formalin, dehydrated, and embedded in paraffin. Sections 0.5 µm thick were placed on poly-Lysine coated slides, deparaffinized, hydrated, and underwent antigen retrieval with 10 mM citrate buffer pH 6.0. They were then blocked with protein block for 10 minutes and incubated with antibodies against Vinculin (1:200), Ki67 (1:200), VEGF (1:100), and CD4 (1:100) at 4°C. Slides were incubated with HRP-polymer quanto for 30 minutes at room temperature and developed using DAB quanto substrate. Counterstaining with hematoxylin followed, and images were captured using an upright Nikon E1 microscope (Nikon Corporation, Tokyo, Japan).

Ki67 and VEGF expression were determined by the optical density of DAB-labeled cells, where DAB-positive staining indicates brown-colored cells. Staining intensity quantification utilized the image processing software Fiji (ImageJ version 2.0) as described by Patera et al. The color deconvolution function was applied to microphotographs, yielding three independent digital images (H&E, DAB, and a complementary image). Stain-specific optical density values were determined, collecting mean grey values from image 2 (DAB). Optical density was then calculated using the formula optical density = log (max grey intensity/mean grey intensity).

4.6. Cloning of luciferase reporter construct and luciferase assay

The 3’UTR sequence of the PHB transcript was obtained from the Ensemble genome browser. The region containing the target site of miR-718 was then amplified from the human genome using primers listed in Table 1. This amplified region was inserted downstream of the renilla luciferase gene, between the Xho1 and Not1 cut sites of the psiCHECK-2 vector (Promega Corporation, Madison, WI), to generate the luciferase reporter construct. The plasmid was verified by sequencing and PCR analysis. For the luciferase assay, HaCaT cells were co-transfected in a 12-well plate. Co-transfection of the luciferase reporter construct (200ng) was performed along with a 40nM dose of either miR-718 or AM-718 or their respective controls. After 24 hours of transfection, a dual luciferase assay (Promega Corporation, MD, USA) was conducted, and luminescence was measured using an Infinite M200 Pro Multimode Reader (TECAN, Männedorf, Switzerland). Renilla luciferase values were normalized to those of firefly luciferase.

4.7. Mitochondrial potential measurement

The mitochondrial membrane potential was assessed following the manufacturer’s protocol (Invitrogen, Oregon, USA). HaCaT cells were cultured in twelve-well plates and transfected with miR-718, M-NC, AM-718, or AM-NC (40 nM). A positive control for depolarization, CCCP (50uM), was included. After 24 hours, the cells were trypsinized, washed with 1X PBS, and stained with JC-1 dye (5 nM) (Invitrogen, Oregon, USA) for 15 minutes at 37°C. Following incubation, the cells were washed, and the fluorescence was measured using a flow cytometer (BD FACS Accuri C6 Plus, NJ, USA). The results are reported as the ratio of red to green fluorescence per 10,000 cells.

4.8. Statistical analysis

All results are expressed as mean ± SEM. The differences between the two groups were analyzed using Student’s two-tailed t-test, with p-values less than 0.05 considered statistically significant.

Abbreviations

JAK - janus kinase

STAT - signal transducer and activator of transcription

IMQ- Imiquimod

MiRNA - microRNA

NF-Kb - Nuclear factor kappa-light-chain-enhancer of activated B cells

IHC - immunohistochemistry

H&E - Hematoxylin and eosin

PHB – prohibitin

MFN1 – mitofusin1

MFN2 – mitofusin2

OPA1 - optic Atrophy 1

DRP1 - dynamin-related protein 1

JC-1 - 5,5,6,6'-tetrachloro- 1,1',3,3'-tetraethylbenzimi-dazoylcarbocyanine iodide

Declarations

Data Availability Statement

Raw data will be available from the corresponding author on request.

Conflict of Interest Statement

The authors declare that there are no conflicts of interest.

Acknowledgements

The authors would like to thank Dr. Vijay Pal Singh, Mr. Amit Misri, and Kiran for their help in animal handling and care. Schematic diagram was created with the help of BioRender.com.

Author contribution statement

Himani Rani: Conceptualization, Methodology, Execution of experiments, Formal Analysis, Data Curation, Writing-original draft, review & editing**. Neeru Saini**: Conceptualization, Methodology, Formal Analysis, Investigation, Supervision; Writing-review & editing, Funding Acquisition.

Funding

Elucidating the role of regulatory gene networks in cellular homeostasis, senescence, and cancer (CSIR OLP-DU5) Himani Rani was supported by CSIR-SRF to conduct the study.

Consent to publication

Authors give consent for publication.

References

1. Michalek, I. M., B. Loring, and S. M. John. 2017. A systematic review of worldwide epidemiology of psoriasis. *Journal of the European Academy of Dermatology and Venereology* 31: 205–212.
2. Deng, Y., C. Chang, and Q. Lu. 2016. The Inflammatory Response in Psoriasis: a Comprehensive Review. *Clin Rev Allergy Immunol* 50: 377–89.
3. Koca, T. T. 2016. A short summary of clinical types of psoriasis. *North Clin Istanb* .
4. Rendon, A., and K. Schäkel. 2019. Psoriasis Pathogenesis and Treatment. *Int J Mol Sci* 20.
5. Alwan, W., and F. O. Nestle. 2015. Pathogenesis and treatment of psoriasis: exploiting pathophysiological pathways for precision medicine. *Clin Exp Rheumatol* 33: S2-6.
6. Hu, X., J. Li, M. Fu, X. Zhao, and W. Wang. 2021. The JAK/STAT signaling pathway: from bench to clinic. *Signal Transduct Target Ther* 6: 402.
7. Wen, Z., Z. Zhong, and J. E. Darnell. 1995. Maximal activation of transcription by Stat1 and Stat3 requires both tyrosine and serine phosphorylation. *Cell* 82: 241–50.
8. Hald, A., R. M. Andrés, M. L. Salskov-Iversen, R. B. Kjellerup, L. Iversen, and C. Johansen. 2013. STAT1 expression and activation is increased in lesional psoriatic skin. *British Journal of Dermatology* 168: 302–310.
9. Johansen, C., A. H. Rittig, M. Mose, T. Bertelsen, I. Weimar, J. Nielsen, T. Andersen, T. K. Rasmussen, B. Deleuran, and L. Iversen. 2017. STAT2 is involved in the pathogenesis of psoriasis by promoting CXCL11 and CCL5 production by keratinocytes. *PLoS One* 12: e0176994.
10. Missiroli, S., I. Genovese, M. Perrone, B. Vezzani, V. A. M. Vitto, and C. Giorgi. 2020. The Role of Mitochondria in Inflammation: From Cancer to Neurodegenerative Disorders. *J Clin Med* 9.
11. Yapa, N. M. B., V. Lisnyak, B. Reljic, and M. T. Ryan. 2021. Mitochondrial dynamics in health and disease. *FEBS Lett* 595: 1184–1204.
12. van der Bliek, A. M., Q. Shen, and S. Kawajiri. 2013. Mechanisms of mitochondrial fission and fusion. *Cold Spring Harb Perspect Biol* 5.
13. Rimessi, A., M. Previati, F. Nigro, M. R. Wieckowski, and P. Pinton. 2016. Mitochondrial reactive oxygen species and inflammation: Molecular mechanisms, diseases and promising therapies. *Int J Biochem Cell Biol* 81: 281–293.
14. Armstrong, A. W., and C. Read. 2020. Pathophysiology, Clinical Presentation, and Treatment of Psoriasis: A Review. *JAMA* 323: 1945–1960.
15. Xu, N., F. Meisgen, L. M. Butler, G. Han, X.-J. Wang, C. Söderberg-Nauclér, M. Ståhle, A. Pivarcsi, and E. Sonkoly. 2013. MicroRNA-31 is overexpressed in psoriasis and modulates inflammatory cytokine and chemokine production in keratinocytes via targeting serine/threonine kinase 40. *J Immunol* 190: 678–88.
16. Guinea-Viniegra, J., M. Jiménez, H. B. Schonthaler, R. Navarro, Y. Delgado, M. J. Concha-Garzón, E. Tschachler, S. Obad, E. Daudén, and E. F. Wagner. 2014. Targeting miR-21 to treat psoriasis. *Sci Transl Med* 6: 225re1.
17. Wu, R., J. Zeng, J. Yuan, X. Deng, Y. Huang, L. Chen, P. Zhang, H. Feng, Z. Liu, Z. Wang, X. Gao, H. Wu, H. Wang, Y. Su, M. Zhao, and Q. Lu. 2018. MicroRNA-210 overexpression promotes psoriasis-like inflammation by inducing Th1 and Th17 cell differentiation. *J Clin Invest* 128: 2551–2568.
18. García-Rodríguez, S., S. Arias-Santiago, J. Orgaz-Molina, C. Magro-Checa, I. Valenzuela, P. Navarro, R. Naranjo-Sintes, J. Sancho, and M. Zubiaur. 2014. Abnormal levels of expression of plasma microRNA-33 in patients with psoriasis. *Actas Dermosifiliogr* 105: 497–503.
19. Chowdhari, S., and N. Saini. 2014. hsa-miR-4516 mediated downregulation of STAT3/CDK6/UBE2N plays a role in PUVA induced apoptosis in keratinocytes. *J Cell Physiol* 229: 1630–8.
20. Sticht, C., C. De La Torre, A. Parveen, and N. Gretz. 2018. miRWalk: An online resource for prediction of microRNA binding sites. *PLoS One* 13: e0206239.
21. Agarwal, V., G. W. Bell, J.-W. Nam, and D. P. Bartel. 2015. Predicting effective microRNA target sites in mammalian mRNAs. *Elife* 4.
22. Rappaport, N., M. Twik, I. Plaschkes, R. Nudel, T. Iny Stein, J. Levitt, M. Gershoni, C. P. Morrey, M. Safran, and D. Lancet. 2017. MalaCards: an amalgamated human disease compendium with diverse clinical and genetic annotation and structured search. *Nucleic Acids Res* 45: D877–D887.
23. Mi, H., and P. Thomas. 2009. PANTHER Pathway: An Ontology-Based Pathway Database Coupled with Data Analysis Tools. In 123–140.
24. Jiang, C.-K., S. Flanagan, M. Ohtsuki, K. Shuai, I. M. Freedberg, and M. Blumenberg. 1994. Disease-Activated Transcription Factor: Allergic Reactions in Human Skin Cause Nuclear Translocation of STAT-91 and Induce Synthesis of Keratin K17. *Mol Cell Biol* 14:

4759–4769.

25. Fu, M., and G. Wang. 2012. Keratin 17 as a therapeutic target for the treatment of psoriasis. *J Dermatol Sci* 67: 161–165.
26. Mezentsev, A., A. Nikolaev, and S. Bruskin. 2014. Matrix metalloproteinases and their role in psoriasis. *Gene* 540: 1–10.
27. Signorile, A., G. Sgaramella, F. Bellomo, and D. De Rasmo. 2019. Prohibitins: A Critical Role in Mitochondrial Functions and Implication in Diseases. *Cells* 8.
28. Legros, F., A. Lombès, P. Frachon, and M. Rojo. 2002. Mitochondrial fusion in human cells is efficient, requires the inner membrane potential, and is mediated by mitofusins. *Mol Biol Cell* 13: 4343–54.
29. Seyhan, A. A. 2024. Trials and Tribulations of MicroRNA Therapeutics. *Int J Mol Sci* 25.
30. Iacomino, G. 2023. miRNAs: The Road from Bench to Bedside. *Genes (Basel)* 14.
31. Kim, T., and C. M. Croce. 2023. MicroRNA: trends in clinical trials of cancer diagnosis and therapy strategies. *Exp Mol Med* 55: 1314–1321.
32. Kalantari, P., O. F. Harandi, S. Agarwal, F. Rus, E. A. Kurt-Jones, K. A. Fitzgerald, D. R. Caffrey, and D. T. Golenbock. 2017. miR-718 represses proinflammatory cytokine production through targeting phosphatase and tensin homolog (PTEN). *Journal of Biological Chemistry* 292: 5634–5644.
33. Leng, R., L. Zha, and L. Tang. 2014. MiR-718 represses VEGF and inhibits ovarian cancer cell progression. *FEBS Lett* 588: 2078–2086.
34. Kim, S. Y., Y. Kim, H. Y. Hwang, and T.-Y. Kim. 2007. Altered expression of prohibitin in psoriatic lesions and its cellular implication. *Biochem Biophys Res Commun* 360: 653–8.
35. Dhillon-LaBrooy, A., K. L. Braband, E. Tantawy, F. Rampoldi, Y.-S. Kao, F. Boukhallouk, L. N. Velasquez, P. Mamareli, L. Silva, L. E. A. Damasceno, B. Weidenthaler-Barth, L. Berod, L. Almeida, and T. Sparwasser. 2024. Inhibition of Mitochondrial Translation Ameliorates Imiquimod-Induced Psoriasis-Like Skin Inflammation by Targeting Vγ4+ γδ T Cells. *J Invest Dermatol* 144: 844-854.e2.

Figures

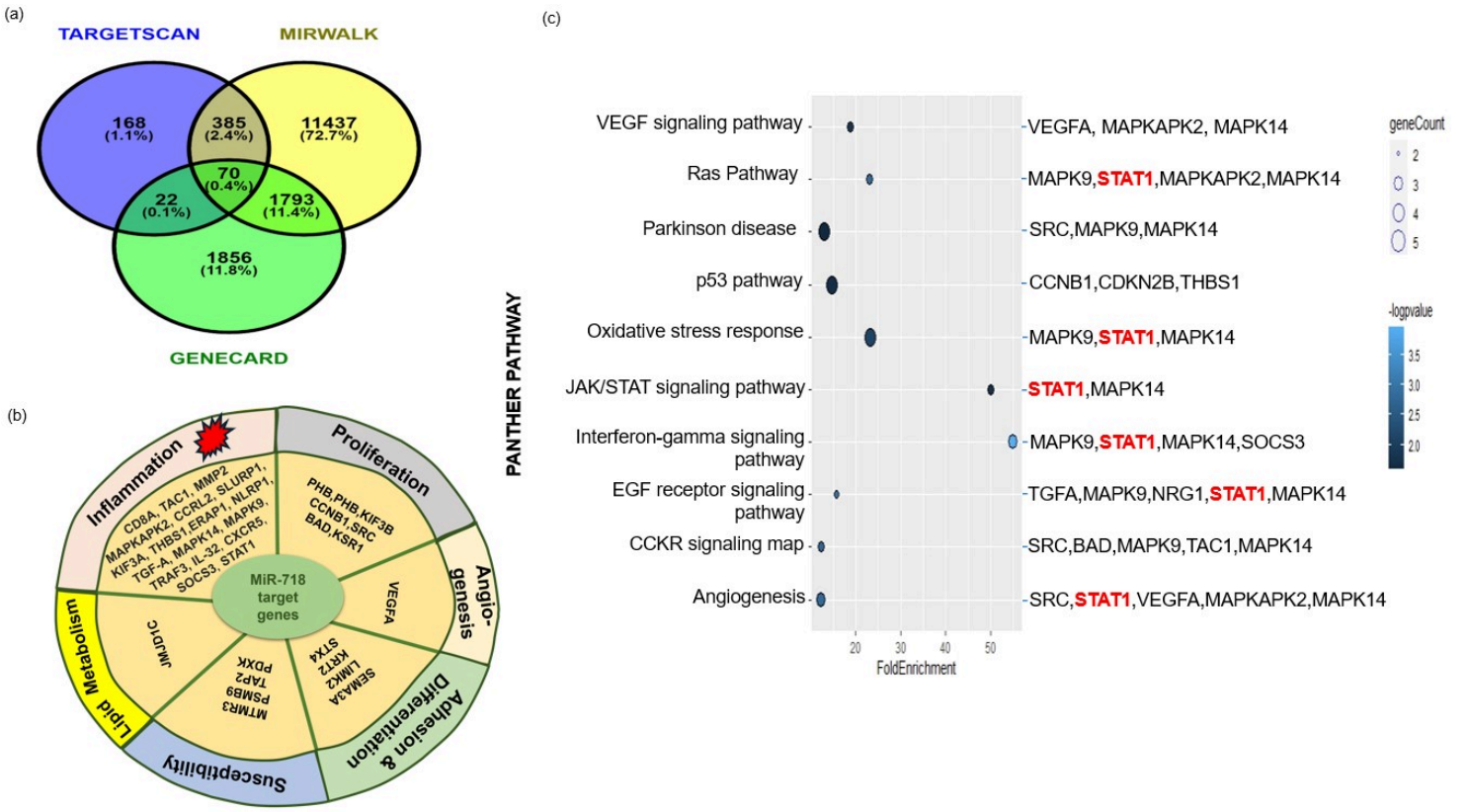

Figure 1

Investigating the Role of miR-718 in Psoriasis: Target Prediction, Pathway Analysis, and STAT1 Interaction Validation

(a) Target genes of miR-718 in psoriasis were predicted using TargetScan and miRWalk, identifying 70 common genes when compared with MalaCards genes. **(b)** These genes were classified into six categories based on their involvement in psoriasis-related pathways identified through PubMed analysis. **(c)** Panther pathway analysis revealed significant involvement of these genes in inflammation-associated pathways, with STAT1 emerging as a key player in most of these pathways.

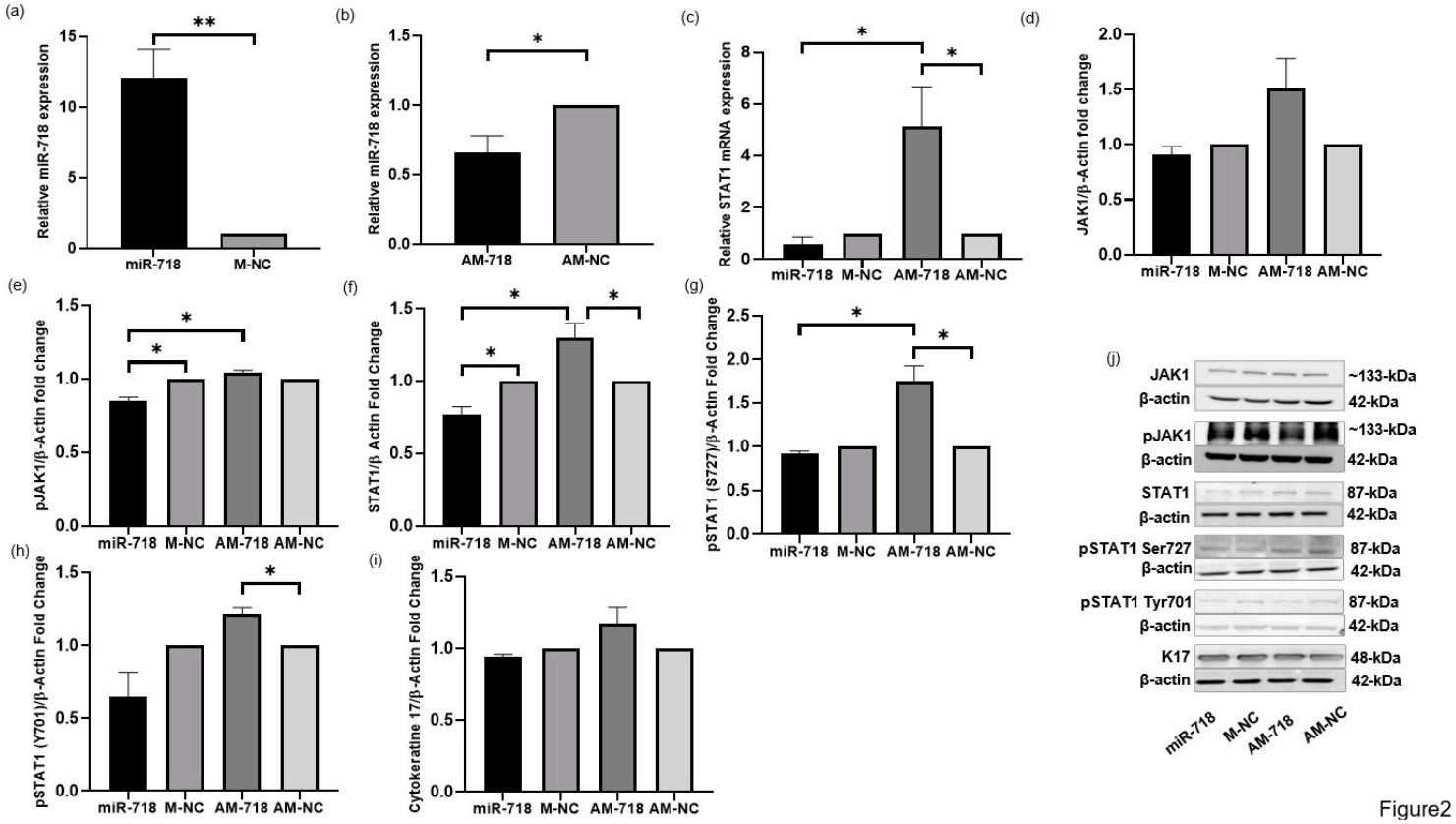

Figure 2

Overexpression of miR-718 Suppresses the Expression of JAK1/STAT1 Proteins in Human Keratinocytes

(a) and **(b)** Quantification of miR-718 expression using SYBR Green master mix after miR-718 and AM-718 transfection in HaCaT cells. M-NC and AM-NC were used for normalization, respectively. **(c)** Relative STAT1 mRNA levels quantified using qRT-PCR with 18S rRNA used for normalization. **(d-i)** Western blot analysis of JAK1, phosphorylated JAK1 (pJAK1), STAT1, phosphorylated STAT1 (Ser727), phosphorylated STAT1 (Tyr701), and Cytokeratin 17 (K17) proteins. Bar graphs represent the integrated densitometry values normalized to β-Actin. **(j)** Representative images of Western blotting. AntimiR-718 mimic = AM-718, miR-718 mimic = miR-718, miR negative control = M-NC, AntimiR negative control = AM-NC. Data are mean ± SEM from three independent experiments, *$p \leq 0.05$, **$p \leq 0.005$.

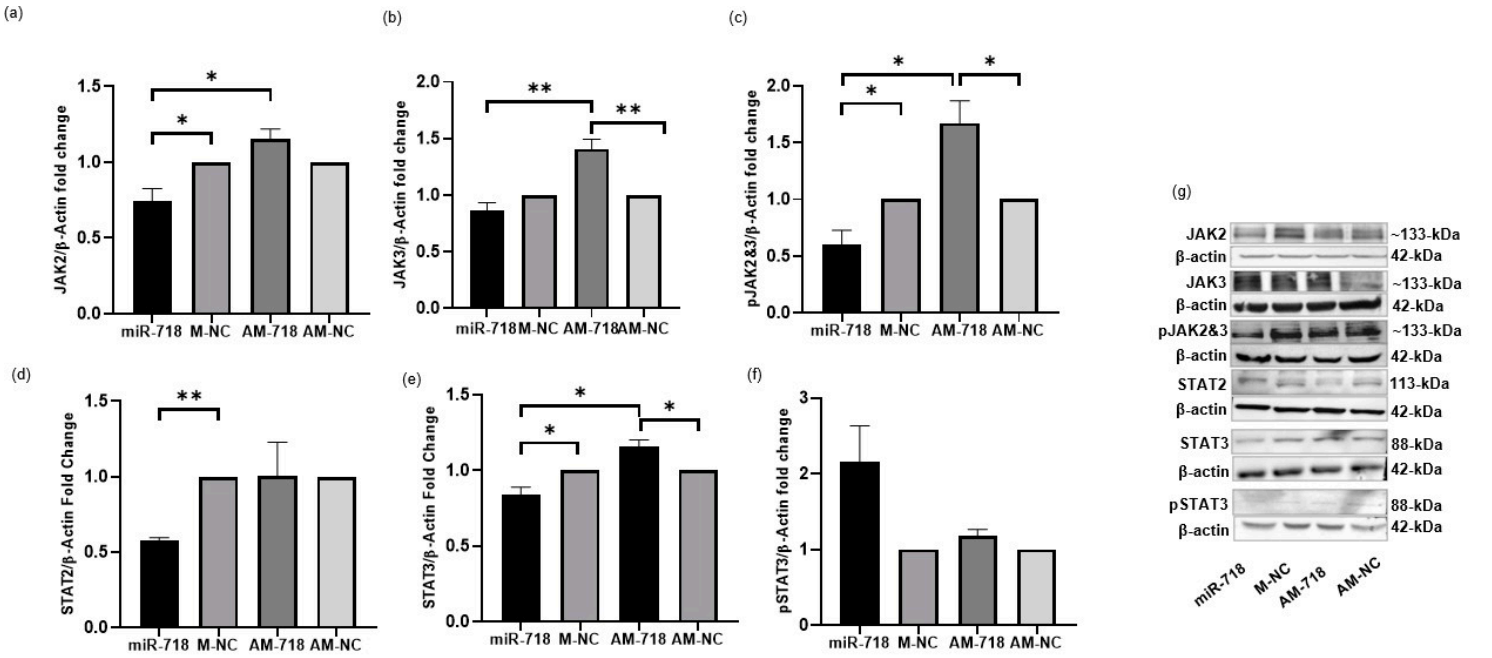

Figure 3

MiR-718 Inhibits JAK/STAT Pathway-Related Proteins, in Addition to STAT1, in HaCaT Cells

Bar graphs of Western blot analysis showing the expression of key molecules of the JAK/STAT signaling pathway, including **(a)** JAK2, **(b)** JAK3, **(d)** STAT2, and **(e)** STAT3, which were significantly inhibited in miR-718 transfected HaCaT keratinocytes. Expression was also analyzed with AM-718 treatment. **(c)** and **(f)**show the expression of phosphorylated JAK2 & JAK3 (pJAK2 & pJAK3) and phosphorylated STAT3 (pSTAT3). **(g)** Representative Western blot images. AntimiR-718 mimic = AM-718, miR-718 mimic = miR-718, miR negative control = M-NC, AntimiR negative control = AM-NC. Data are mean ± SEM from three independent experiments, *p ≤ 0.05, **p ≤ 0.005.

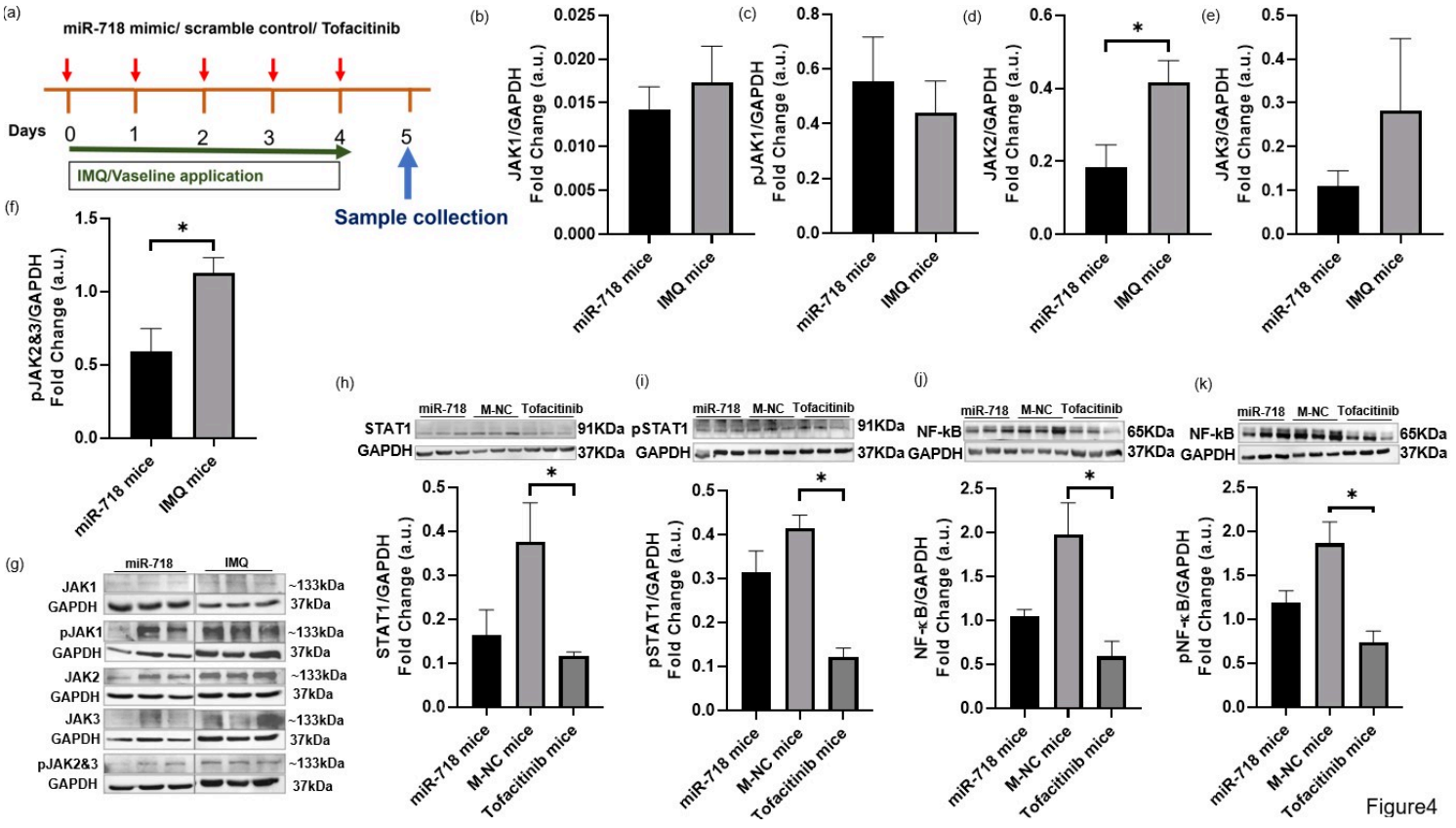

Figure 4

Inhibition of JAK/STAT1 Signaling in IMQ-Induced Psoriatic Mice Model Due to miR-718 Overexpression

(a) Timeline illustrating the preparation of the IMQ-induced psoriasis mice model and the administration of different treatments in mice (n=5). **(b-f)** JAK protein expression, **(h-i)** STAT1 protein expression, and **(j-k)** NF-kB protein expression were analyzed using Western blotting. Protein expression values were normalized to GAPDH and plotted. **(f)** Representative blot images of JAK1, pJAK1, JAK2, JAK3, pJAK2 & pJAK3. The bar graph represents the mean ± SEM from three mice per treated group, *p ≤ 0.05, **p ≤ 0.005. IMQ = IMQ-induced psoriatic mice, miR-718 = miR-718 intradermal injection along with IMQ topical application, M-NC = scramble oligonucleotides intradermal injection along with IMQ topical application, tofacitinib = tofacitinib (30 mg/kg) oral treatment along with IMQ topical application.

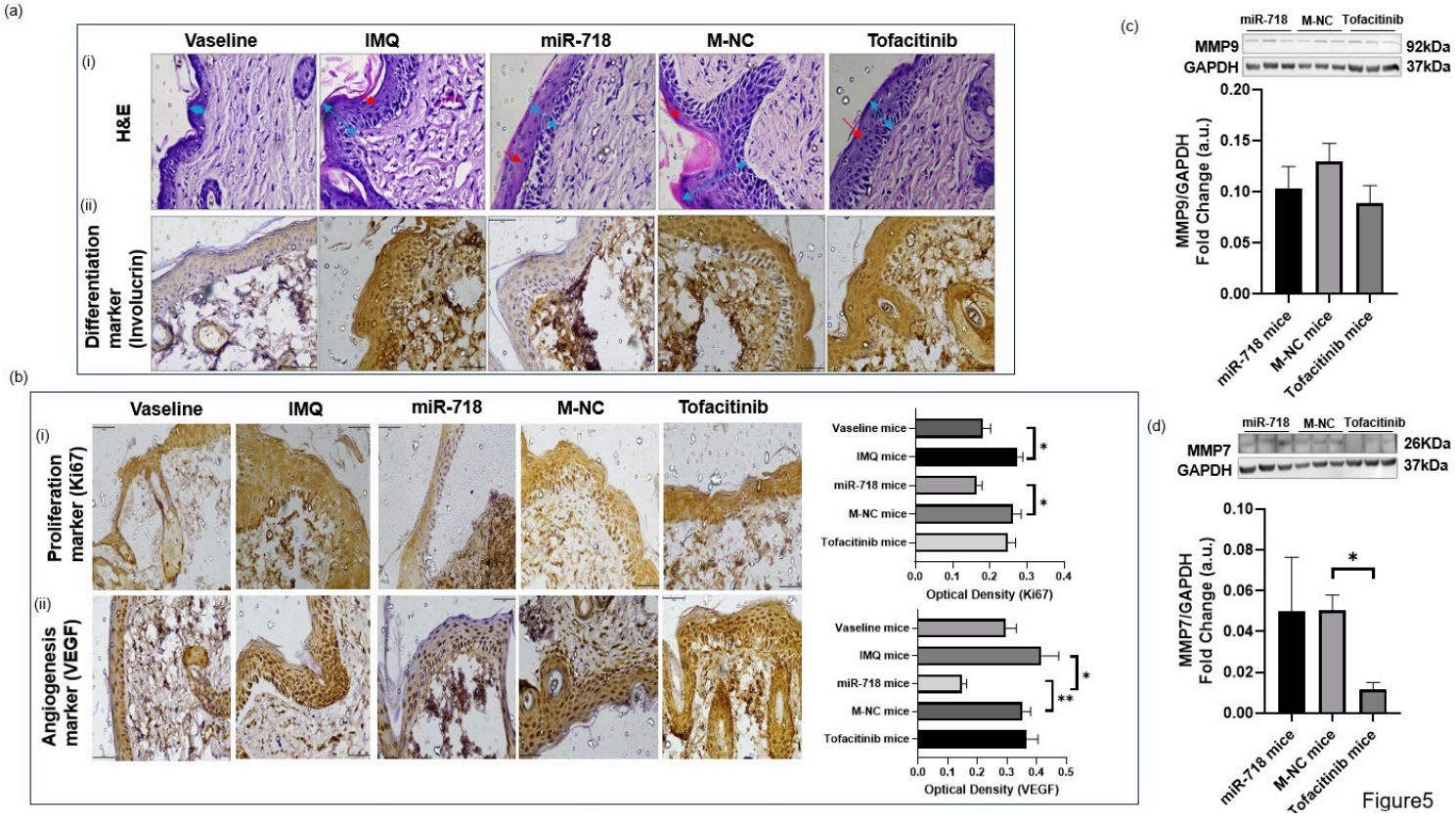

Figure 5

Modification of Psoriatic-Like Symptoms Through the Upregulation of miR-718 in Psoriatic Skin of Mice

(ai) Representative H&E-stained sections of mice skin from different experimental groups showing increased cell number (hyperplasia), thickness of the stratum corneum (hyperkeratosis), indicated by double-headed yellow arrows, and flattened keratinocyte nuclei within the stratum corneum (parakeratosis) indicated by red arrows. **(aii)** DAB-based IHC stained images indicating the involucrin differentiation marker. **(bi)** Evaluation of epidermal proliferation using the Ki67 marker, highlighting decreased keratinocyte proliferation. **(bii)** Histological observations showing reduced VEGF expression in miR-718 treated mice skin, both in IHC images and quantification. Images captured at 40x magnification. Scale bar = 50 µm. The bar graph represents the mean ± SEM from three mice per treated group, *p ≤ 0.05, **p ≤ 0.005. **(c-d)** Western blot analysis of MMP9 and MMP7 expression in mice skin. Vaseline = Vaseline-treated mice (normal mice), IMQ = IMQ-induced psoriatic mice, miR-718 = miR-718 intradermal injection along with IMQ topical application, M-NC = scramble oligonucleotides intradermal injection along with IMQ topical application, tofacitinib = tofacitinib (30 mg/kg) oral treatment along with IMQ topical application.

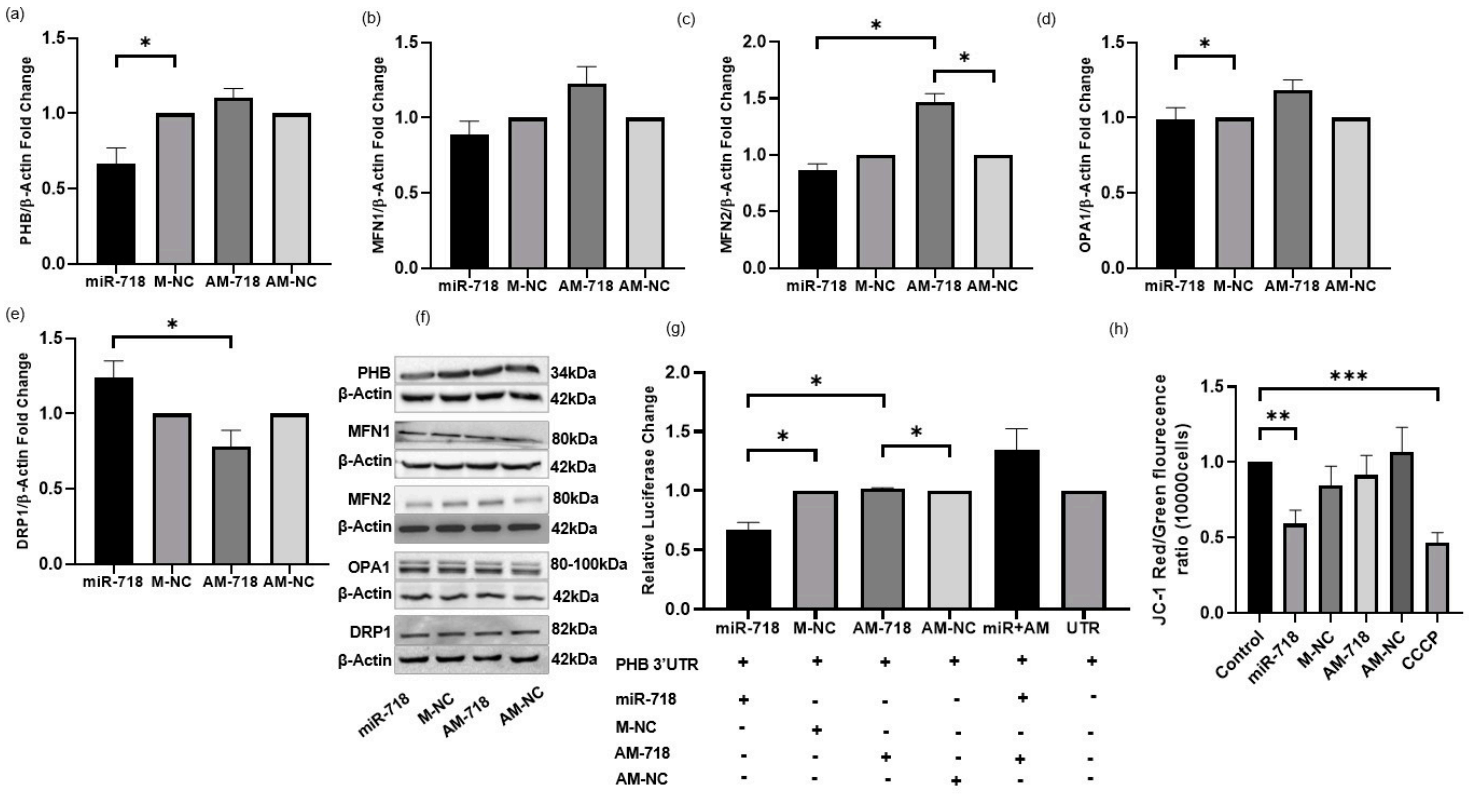

Figure 6

miR-718 Overexpression Effects on Mitochondrial Dynamics and Integrity in HaCaT Cells

Bar graph of Western blot analysis showing the expression of key molecules of mitochondrial dynamics, including **(a)** PHB, **(b)**MFN1, **(d)** MFN2, **(e)** OPA1, and **(f)** DRP1, which were significantly inhibited in miR-718 transfected HaCaT keratinocytes. Expression was also analyzed with AM-718 treatment. **(g)** Luciferase activity measured in HaCaT keratinocytes co-transfected with PHB 3' UTR and either miR-718, M-NC, AM-718, or AM-NC. **(h)** Mitochondrial membrane potential assessment using JC-1 staining. The control group showed a high red/green fluorescence ratio indicating intact mitochondria, which was reversed with CCCP treatment (positive control), showing completely depolarized mitochondria with a low red/green ratio. miR-718 treated cells showed a lower red/green ratio compared to AM-718, indicating mitochondrial fusion upon miR-718 overexpression. **(f)** Representative Western blot images. AntimiR-718 mimic = AM-718, miR-718 mimic = miR-718, miR negative control = M-NC, AntimiR negative control = AM-NC. Data are mean ± SEM from three independent experiments, *$p \leq 0.05$, **$p \leq 0.005$.

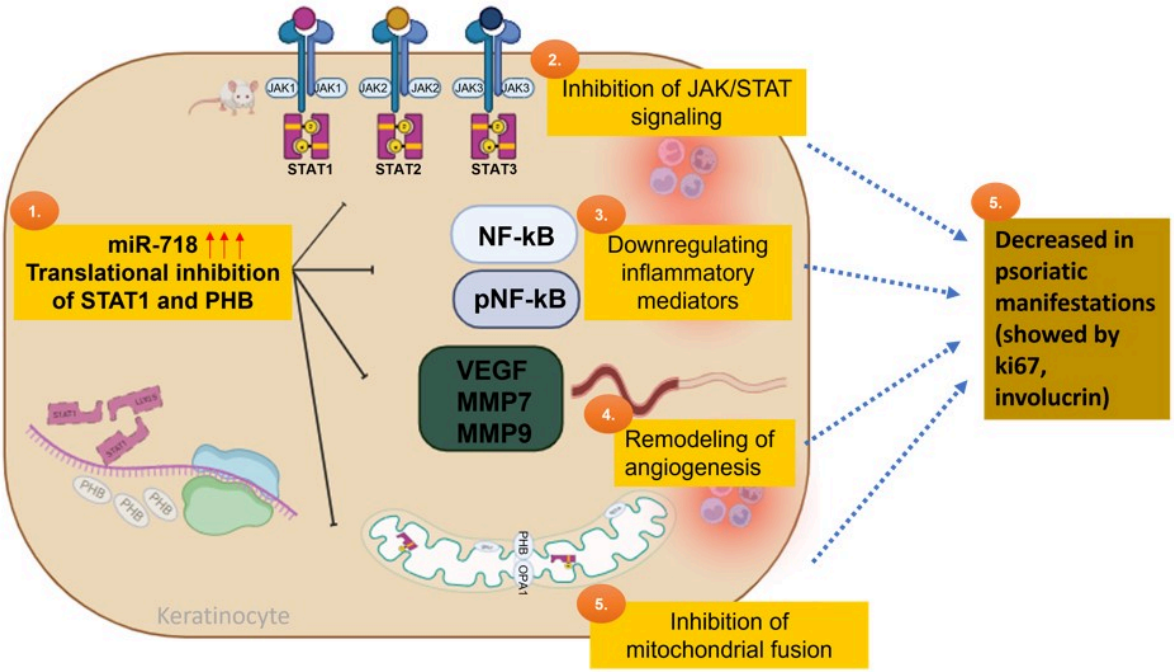

Figure 7

Summary of the Study

(1) miR-718 binds to the STAT1 and PHB mRNA and inhibits their translation.

(2) Overexpression of miR-718 led to the inhibition of the JAK/STAT signaling pathway. This was demonstrated by a decrease in the expression of key signaling molecules, including STAT1, JAK1, JAK2, and JAK3, both in-vivo and in-vitro.

(3) In-vivo studies showed that miR-718 decreased the expression of critical mediator of inflammation, NF-kB and its phosphorylated form.

(4) In miR-718 transfected mouse skin, there was reduction of VEGF (a key factor in angiogenesis) and matrix metalloproteases (MMP7 and MMP9, both of which involved in tissue remodeling and inflammation.

(5) miR-718 regulates mitochondrial dynamics by inhibiting proteins involved in this process (PHB, MFN1, MFN2, OPA1).

(6) The inhibition of the JAK/STAT and NF-kB pathways, reduction of angiogenesis, and regulation of mitochondrial dynamics collectively highlight miR-718 as a promising candidate for psoriasis therapy.

Supplementary Files

This is a list of supplementary files associated with this preprint. Click to download.

- supplementaryfig.pptx
- supplementarytable1.docx
- uncroppedblots13062024.pptx